Femtosecond pulse shaping using a two-dimensional liquid-crystal spatial light modulator

E. Frumker* and Y. Silberberg

Department of Physics of Complex Systems, Weizmann Institute of Science, Rehovot 76100, Israel
**Corresponding author: evgenyf@weizmann.ac.il*

Received January 5, 2007; revised March 11, 2007; accepted March 12, 2007;
posted March 14, 2007 (Doc. ID 78724); published April 25, 2007

We introduce a programmable, high-rate scanning femtosecond pulse shaper based on a two-dimensional liquid crystal on a silicon spatial light modulator (SLM). While horizontal resolution of 1920 addressable pixels provides superior fidelity for generating complex waveforms, scanning across the vertical dimension (1080 pixels) has been used to facilitate at least 3 orders of magnitude speed increase as compared with typical liquid-crystal SLM-based pulse shapers. An update rate in excess of 100 kHz is demonstrated.

OCIS codes: 320.0320, 190.0190, 320.2250, 320.5540, 320.7160, 190.7110.

Fourier-domain femtosecond pulse shaping [1] continues to play a key role in ultrafast sciences. Many applications emerged due to progress made in pulse-shape synthesis. These include, among others, nonlinear spectroscopy and microscopy [2,3], selective femtochemistry and quantum coherent control [4,5], optical communications [6], and high field physics. In many cases, high-speed dynamic pulse-shape control is of primary importance. For example, in many adaptive techniques, browsing through the searchable space of parameters of the waveforms requires numerous iterations, and the pulse-shape update speed is often the rate-limiting element. In another example, fast switching between pulse shapes enables a lock-in microscopy technique [7], where the fast speed is critical to minimize noise and achieve high-resolution real-time imaging. These and other applications prompted the development of a variety of approaches for dynamic Fourier-domain femtosecond pulse shaping. These included usage of one-dimensional (1D) liquid-crystal (LC) spatial light modulators (SLMs) [8], acousto-optic modulators [9], deformable mirrors [10], scanning over fixed masks [7], and electro-optical phased array modulators [11].

In the most ubiquitous approach, a 1D array of LC elements is placed in the Fourier plane of the shaper [8]. This approach is often limited to a few tens of hertz by the slow relaxation rate of the nematic LC. In acousto-optic modulators, the acoustics grating wave is constantly moving in the modulator's aperture. Although for every single femtosecond pulse the acoustic wave appears frozen on the time scale of the pulse itself, the mask pattern changes on the time scale between successive pulses of a typical mode-locked oscillator. In fact, this restricts the usage of acousto-optic modulators to lower repetition rate sources such as femtosecond amplifiers. A deformable mirror shaper [10] is able to provide only smoothly varying phase modulation due to the upper limit on curvature that can be induced in the membrane mirror. The scanning femtosecond pulse shaping [7] allows pulse shapes to be modulated at kilohertz rates but limits them to a predetermined set of static waveforms. Electro-optical gallium arsenide optical phased array modulators [11] provide a very high resolution and unsurpassed update rate on the nanosecond scale, but gallium arsenide has significant absorption at 800 nm, which makes it incompatible with Ti:sapphire laser sources.

In this Letter, we describe a pulse shaper based on two-dimensional (2D) LC on silicon (LCOS) SLM. Two-dimensional LC modulators were already used in Fourier-domain pulse shaping by the Nelson group [12,13]. In their scheme, the horizontal dimension of the SLM was used to encode the spectral pulse-shape data, while the vertical dimension of the 2D SLM was used for real-space or wave-vector encoding [14]. Here we show that the second dimension could be used to significantly improve the modulation speed and the updatability of the generated waveforms. We demonstrate higher than a 100 kHz modulation speed, more than 3 orders of magnitude faster than a typical LC-based shaper, while deploying 1920 programmable pixels for spectral phase pulse-shape data encoding. The presented concept paves the way toward megahertz rates modulation using 2D LC SLMs.

Our 2D LCOS shaper setup arrangement is shown in Fig. 1. The incident beam is reflected from the scanning mirror (SM) and is imaged by the telescope composed of lenses L1 and L2 ($f=100$ mm) onto a diffraction grating G (1200 mm^{-1}). The closed-loop scanner (CTI Model 6220) provides a feedback reading of the instantaneous angular position of the SM. This reading can be used for independent control of scanning amplitude and frequency as well as provide the reference signal for the pulse-shape lock-in detection [7]. The diffracted beam, reflected close to the Littrow angle, is directed by mirror M2 into the Fourier pulse-shaper system composed of the spherical Fourier lens FL ($f=100$ mm) and LCOS SLM (Holoeye Model HEO1080P) in the Fourier plane. The LCOS SLM has 1920×1080 pixels with a pixel pitch of 8 μm and a fill factor of almost 90%. The phase

0146-9592/07/111384-3/$15.00

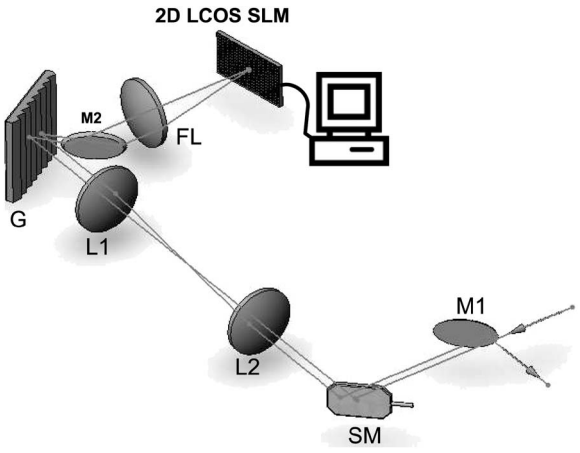

Fig. 1. Schematic of the 2D LCOS SLM pulse shaper.

modulation SLM was checked and calibrated using a Michelson interferometer. It was found to provide a more than 2.5π phase modulation at 827 nm. The parasitic amplitude modulation did not exceed 4% over the entire phase modulation range, hence we can consider the device as a phase-only filter. The SLM was tilted slightly about the vertical axes, so that the zero-diffraction-order reflection was intercepted after the scanner with mirror M1. This tilt does not distort the pulse shape since it is equivalent to a linear spectral phase or a simple shift in the time domain.

There are three main routes to achieve dynamic pulse-shape control with our shaper. In the first scheme, the SM is kept fixed and the updatability is achieved by refreshing the images on the SLM, as in a conventional LC-based shaper. This classical scheme provides very high pulse synthesis fidelity with 1920 addressable pixels for spectral components modulation but is limited by the slow update rate of the nematic LC, 60 Hz as stated by the manufacturer in our case; we experimentally found a 3 ms rise time.

In the second scheme, we divide the SLM into horizontal stripes. Each stripe encodes spectral phase information for a desired pulse shape. The stripe width is, of course, limited by the pixel size, but practically it was kept wider than the spot size in the Fourier plane. By rotating the SM, we sweep the horizontally diffracted spectral components in the vertical direction across the programmed stripes, thereby producing a multitude of different pulse shapes. In this scheme, the pulse-shape update rate f_{pulse} is given by $f_{\text{pulse}}=2*f_{\text{scan}}*(A/d_{\text{stripe}}-1)$, where f_{scan} is the SM frequency, A is scanning peak-to-peak amplitude and d_{stripe} is the stripe width. As the f_{scan} is typically an order of magnitude larger than the typical refresh rate of the SLM, the highest pulse update rate f_{pulse} is achieved by keeping the stripe pattern fixed while scanning the mask. A straightforward combination of these two techniques can be particularly useful for a variety of nonlinear microscopy or spectroscopy applications. A slow SLM update can be used to change the pattern, while the very fast scanning pulse-shape update can enable lock-in detection by switching between shapes [7].

Finally, it is possible to synchronize the SM position with the SLM refresh, so that each scan gets a new set of phase patterns. Although this approach would be slower by factor $[f_{slm}/2f_{\text{scan}}]$ (where f_{slm} is the LC SLM refresh rate) as compared with the previous one, it facilitates generating completely arbitrary waveforms at a rate faster than f_{slm} alone by a factor of twice the number of dynamically encoded stripes. This could provide at least 2 orders of magnitude speed increase over the LC SLM alone. This scheme would be particularly suitable for adaptive techniques, which require numerous iterations for finding an optimal solution.

In all experiments described below, we used a home-built oscillator centered at 800 nm with a 30 nm spectral bandwidth. In the first experiment, we checked the pulse-shaping capability of the system. First we simply encoded a phase pattern to compensate for the residual dispersion experienced by the beam as it passes through the many dispersive elements in our setup. This is done by maximizing a second-harmonic signal from a 20 μm β-barium borate crystal, while searching for the spectral phase polynomial containing group-velocity and third-order dispersion terms with a direct search algorithm. The results, compared by cross correlation with the input pulse, are shown in Fig. 2(a).

The dashed curve is the cross correlation with no phase encoded in the SLM. One can see the asymmetric feature that is typical for third-order dispersion. The solid curve corresponds to the cross-correlation result after the dispersion is compensated. The signal is more symmetric and has practically transform-limited duration, taking into account the geometry of the noncollinear cross-correlation setup. We then encoded a sinusoidal phase pattern $\phi(\omega)=A\sin(B\omega+C)$ into the SLM. In the time domain, this harmonic periodic phase modulation results in a series of pulses with amplitudes proportional to $J_n(A)$ for the nth pulse. The finite spot size in the Fourier plane causes additional apodization of the intensity distribution of the output

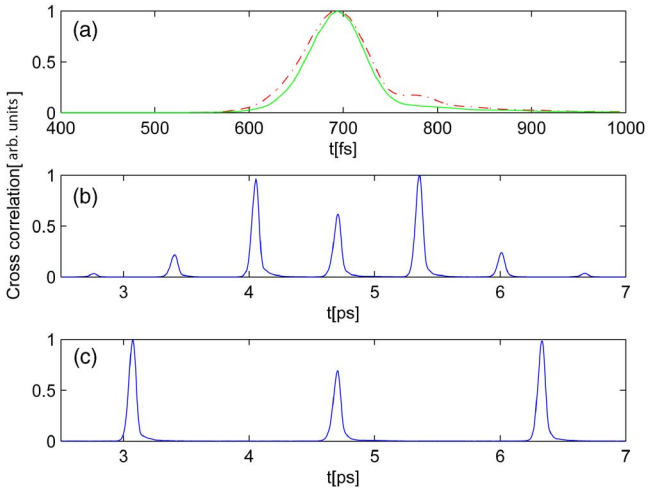

Fig. 2. (Color online) Experimental cross-correlation results. (a) Before (dashed curve) and after (solid curve) dispersion correction. Sinusoidal spectral phase encoded into SLM period (b) 1.55 and (c) 0.62 THz.

pulses [1]. Typical results are shown in Figs. 2(b) and 2(c) for periods of ~1.55 and 0.62 THz, respectively. The distance between the pulses in the time domain was found to be 646 fs and 1.62 ps respectively, as expected.

To check the update rate of the shaper, we encoded two types of alternating horizontal stripes. One stripe contained the spectral phase needed for dispersion correction that led to a transform-limited pulse. The other stripe was encoded with a sinusoidal spectral phase with a period of ~1.55 THz. We verified that this periodic modulation reduces the second-harmonic generation (SHG) signal by more than factor of 4 as compared with the transform-limited pulse, while the light intensity was reduced by less than 2%. The entire 2D aperture of the SLM was filled with these alternating stripes mask. We then scanned the mirror with a triangle modulation signal to guarantee equal time spacing. The positioning and the current feedback available from the scanner was monitored by a digital oscilloscope along with the photomultiplier tube output measuring the SHG signal. The photomultiplier tube output was amplified with the low-noise preamp Model SRS560 and acquired by the oscilloscope in the averaging mode (100 times) to reduce the noise.

In Fig. 3(a), the resulting SHG signal is shown as a function of time. In this case, the scanning mirror frequency was set to 2200 Hz and the stripe width was 6 pixels (~50 μm). The pulse-shape update rate achieved in this case is ~140 kHz, which is at least 3 orders of magnitude faster than the best LC SLMs. In this particular case, the stripe width was close to the spot size in the Fourier plane (~30 μm). Intersection of this spot with the edges of the stripe causes diffraction and reduction of the SHG signal. This explains the relatively sharp peaks in Fig. 3(a). Note the difference between the 6 pixel width with a 960 Hz scanning frequency and a 12 pixel width with 1920 Hz shown in Figs. 3(b) and 3(c), respectively. While both cases result in the same modulation frequency of ~62 kHz, the 6 pixel width case has consistently sharper peaks.

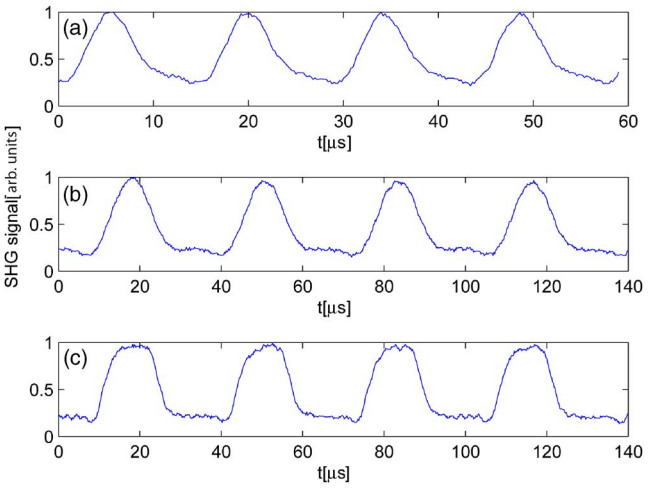

Fig. 3. (Color online) Update speed measurements. (a) Scanning rate 2200 Hz, 6 pixels stripe width. (b) Scanning rate 960 Hz, 6 pixels stripe width. (c) Scanning rate 1920 Hz, 12 pixels stripe width.

In summary, we have introduced a pulse-shaping technique based on a 2D LC SLM. The concept provides at least an additional 3 orders of magnitude speed increase over a typical LC SLM shaper, while providing very high fidelity in pulse-shape synthesis. We believe that the unique combination of extremely fast speed, very high fidelity, and robustness could have a significant impact in diverse fields of femtosecond research. A combination of this technique with faster scanning polygon mirrors may lead to megahertz update rate shaping. Usage of a micromirror SLM [15] instead of a LC SLM in the combined scheme for arbitrary waveforms generation will lead to at least another order of magnitude update rate increase.

We gratefully acknowledge financial support by The Israeli Academy of Science and by the Israeli Ministry of Science. Y. Silverberg holds the Harry Weinrebe Professorial chair of Laser Physics.

References

1. A. M. Weiner, Rev. Sci. Instrum. **71**, 1929 (2000).
2. P. Tian, D. Keusters, Y. Suzaki, and W. S. Warren, Science **300**, 1553 (2003).
3. N. Dudovich, D. Oron, and Y. Silberberg, Nature **418**, 512 (2002).
4. A. Assion, T. Baumert, M. Bergt, T. Brixner, B. Kiefer, V. Seyfried, M. Strehle, and G. Gerber, Science **282**, 919 (1998).
5. D. Meshulach and Y. Silberberg, Nature **396**, 239 (1998).
6. A. M. Weiner, J. P. Heritage, and J. A. Salehi, Opt. Lett. **13**, 300 (1988).
7. E. Frumker, D. Oron, D. Mandelik, and Y. Silberberg, Opt. Lett. **29**, 890 (2004).
8. A. M. Weiner, D. E. Leaird, J. S. Patel, and J. R. Wullert II, Opt. Lett. **15**, 326 (1990).
9. C. W. Hillegas, J. X. Tull, D. Goswami, D. Strickland, and W. S. Warren, Opt. Lett. **19**, 737 (1994).
10. E. Zeek, K. Maginnis, S. Backus, U. Russek, M. Murnane, G. Mourou, H. Kapteyn, and G. Vdovin, Opt. Lett. **24**, 493 (1999).
11. E. Frumker, E. Tal, Y. Silberberg, and D. Majer, Opt. Lett. **30**, 2796 (2005).
12. M. M. Wefers, K. A. Nelson, and A. M. Weiner, Opt. Lett. **21**, 746 (1996).
13. T. Feurer, J. C. Vaughan, and K. A. Nelson, Science **299**, 374 (2003).
14. T. Feurer, J. C. Vaughan, R. M. Koehl, and K. A. Nelson, Opt. Lett. **27**, 652 (2002).
15. M. Hacker, G. Stobrawa, R. Sauerbrey, T. Buckup, M. Motzkus, M. Wildenhain, and A. Gehner, Appl. Phys. B **76**, 711 (2003).